Localized nonlinear matter waves in two-component Bose-Einstein condensates with time- and space-modulated nonlinearities

Deng-Shan Wang,[1,2] Xing-Hua Hu,[1] and W. M. Liu[1]

[1]*Beijing National Laboratory for Condensed Matter Physics, Institute of Physics, Chinese Academy of Sciences, Beijing 100190, People's Republic of China*

[2]*CEMA, Central University of Finance and Economics, Beijing 100081, People's Republic of China*

(Received 11 May 2010; revised manuscript received 13 July 2010; published 20 August 2010)

We investigate the localized nonlinear matter waves in the two-component Bose-Einstein condensates with time- and space-modulated nonlinearities analytically and numerically. The similarity transformations are developed to solve the coupled Gross-Pitaevskii equations and two families of explicitly exact solutions are derived. Our results show that not only the attractive spatiotemporal inhomogeneous interactions but the repulsive ones support novel localized nonlinear matter waves in two-component Bose-Einstein condensates. The dynamics of these matter waves, including the breathing solitons, quasibreathing solitons, resonant solitons, and moving solitons, is discussed. We confirm the stability of the exact solutions by adding various initial stochastic noise and study the general cases of the interaction parameters numerically. We also provide the experimental parameters to produce these phenomena in future experiments.

DOI: 10.1103/PhysRevA.82.023612 PACS number(s): 03.75.Lm, 05.45.Yv, 42.65.Tg

I. INTRODUCTION

The realization of Bose-Einstein condensations (BECs) in weakly interacting atomic gases [1] has opened the possibility to investigate nonlinear properties of atomic matter waves. Several remarkable phenomena [2], which strongly resemble well-known effects in nonlinear optics, have been observed in BECs. In recent years, the development of trapping techniques has allowed the creation of two-component BECs [3–5], which are formed by trapping atoms in different internal states [6,7]. The two-component BECs, far from being a trivial extension of the single-component one, present novel and fundamentally different scenarios for its ground state [8] and excitations [9]. The theory for a two-component condensate can be developed similarly to that for a one-component condensate whose equilibrium and dynamical properties can be accurately described by the Gross-Pitaevskii (GP) equations [3–9].

In past decades, techniques for managing nonlinearity have attracted considerable attention. For instance, nonlinearity management arises in optics for transverse beam propagation in layered optical media as well as in atomic physics for the Feshbach resonance [10] of the scattering length of interatomic interactions in BECs. In these situations, one has to deal with the governing equations with the nonlinearity coefficients being functions of time [11]. In recent researches, the space-dependent [12,13] or spatiotemporal-dependent [14] nonlinearities are considered by similarity transformations, and some explicitly exact solutions of the single nonlinear Schrödinger equations [15] are constructed. However, there is little work considering the dynamics of the two-component BECs with time- and space-modulated nonlinearities.

In this paper we study the localized nonlinear matter waves in the two-component BECs with time- and space-modulated nonlinearities in harmonic potential. To do so, we make use of the similarity transformations that connect problems with time- and space-modulated nonlinearities with simpler ones that have an homogeneous nonlinearity. We show that in the two-component BECs, not only the attractive spatially inhomogeneous interactions but the repulsive ones can support novel localized nonlinear matter waves. We also find that the localized nonlinear matter waves have the behaviors of breathing solitons, quasibreathing solitons, resonant solitons, and moving solitons. Numerical simulations are used to show the stability of our exact solutions and the dynamics of the two-component BECs with general cases of the interaction parameters. In addition, we provide the experimental parameters to produce these phenomena in future experiments. These are interesting results with potential physical implications.

II. THE THEORETICAL MODEL

The two interacting dilute Bose condensates can be well described by the zero-temperature mean-field theory, in which the collisions between the condensate atoms and the thermal cloud are neglected. Considering two-component BECs each of mass m_a trapped in an external potential, the mean-field dynamics can be derived by assuming that the two condensates are described by the wave functions $\Psi_1(\mathbf{r},t)$ and $\Psi_2(\mathbf{r},t)$. At low temperature, the total-energy functional of the system is

$$E[\Psi_1,\Psi_2] = \int d\mathbf{r}\left(\frac{\hbar^2}{2m_a}|\Delta\Psi_1|^2 + \frac{\hbar^2}{2m_a}|\Delta\Psi_2|^2 + V_{\rm ext}^{(1)}|\Psi_1|^2 + V_{\rm ext}^{(2)}|\Psi_2|^2 + \frac{1}{2}U_1|\Psi_1|^4 + \frac{1}{2}U_2|\Psi_2|^4 + U_{12}|\Psi_1|^2|\Psi_2|^2\right). \quad (1)$$

Here the trapping potentials are assumed to be $V_{\rm ext}^{(i)} = m_a[\omega_{i\perp}^2(\gamma_i^2x^2 + y^2 + z^2)]/2, i = 1,2,$ where $\gamma_i = \omega_{ix}/\omega_{i\perp}$ conveniently parametrizes the trap anisotropy, and $\omega_{i\perp}$ and ω_{ix} are the the confinement frequencies in the transverse and axial directions. The intracomponent coupling constant $U_i = 4\pi\hbar^2a_{ii}/m_a$ is characterized by the scattering lengths a_{11} and a_{22} between atoms of the same species, while the intercomponent coupling constant $U_{12} = 4\pi\hbar^2a_{12}/m_a$ is determined by the scattering length a_{12} where an atom in the Ψ_1 component scatters from another atom in the Ψ_2 component.

In this paper we consider the scattering lengths a_{11},a_{22}, and a_{12} to be spatiotemporally inhomogeneous [12–14], which is experimentally feasible due to the flexible and precise control of the scattering lengths achievable in quasi-one-dimensional BECs with magnetically tuning the Feshbach resonances.

The dynamics of the two-component BECs is governed by coupled dimensionless GP equations, which are derived from the variational principle $i\hbar\partial\Psi_i/\partial t = \delta E/\delta\psi_i^*$ as shown in [3–9]

$$i\hbar\frac{\partial\Psi_1}{\partial t} = \left(-\frac{\hbar^2\nabla^2}{2m_a} + V_{\rm ext}^{(1)} + U_1|\Psi_1|^2 + U_{12}|\Psi_2|^2\right)\Psi_1,$$
$$i\hbar\frac{\partial\Psi_2}{\partial t} = \left(-\frac{\hbar^2\nabla^2}{2m_a} + V_{\rm ext}^{(2)} + U_{12}|\Psi_2|^2 + U_2|\Psi_2|^2\right)\Psi_2,$$

where the condensate wave functions are normalized by the particle number $N_i = \int d^3\mathbf{r}|\Psi_i|^2$. If the condensates are tightly confined in the transverse direction, that is $\omega_{i\perp} \gg \omega_{ix}$, i.e., $\gamma_i \ll 1$, it is reasonable to reduce the GP equations for the condensate wave functions to a quasi-one-dimensional system. To do this, one can factorize the condensate wave functions into a longitudinal and a transverse part as

$$\Psi_i(\mathbf{r},t) = \phi_\perp^{(i)}(y,z)\psi_i(x,t)e^{-i\omega_\perp t}, \quad i = 1,2$$

where we assume $\omega_{1\perp} = \omega_{2\perp} = \omega_\perp$, $\omega_{1x} = \omega_{2x} = \omega_x$ to reduce the number of the parameters, and $\phi_\perp^{(i)}(y,z)$ is the normalized ground state of the transverse potential with energy $\hbar\omega_\perp$. Integrating along the transverse coordinates, the resulting equations for the axial wave functions $\psi_{1,2}(x,t)$ in dimensionless form can be written as the coupled quasi-one-dimensional (quasi-1D) GP equations [4,5]

$$i\frac{\partial\psi_1}{\partial t} = \left(-\frac{1}{2}\frac{\partial^2}{\partial x^2} + \frac{\gamma^2}{2}x^2 + b_{11}|\psi_1|^2 + b_{12}|\psi_2|^2\right)\psi_1,$$
$$i\frac{\partial\psi_2}{\partial t} = \left(-\frac{1}{2}\frac{\partial^2}{\partial x^2} + \frac{\gamma^2}{2}x^2 + b_{12}|\psi_1|^2 + b_{22}|\psi_2|^2\right)\psi_2, \tag{2}$$

where $b_{11} = 2a_{11}$, $b_{22} = 2a_{22}$, $b_{12} = 2a_{12}$, and the units for length and time are $\sqrt{\hbar/(m_a\omega_\perp)}$ and $\omega_\perp^{-1}$, respectively.

Model (2) has attracted a great deal of attention due to its applications in the theory of low-dimensional condensed quantum gases. We will construct the explicitly exact solutions of this model under the special interaction parameters b_{11}, b_{12}, and b_{22}, and investigate their unique dynamics.

III. SIMILARITY TRANSFORMATION AND ANALYTIC SOLUTIONS

In this section we consider the exact spatially localized solutions of Eqs. (2) for which $\lim_{|x|\to\infty}\psi_{1,2}(x,t) = 0$. To do this, we take the similarity transformation

$$\psi_1(x,t) = \beta_1(x,t)e^{i\alpha_1(x,t)}U[X(x,t)], \tag{3a}$$
$$\psi_2(x,t) = \beta_2(x,t)e^{i\alpha_2(x,t)}V[X(x,t)], \tag{3b}$$

to reduce Eqs. (2) to two stationary nonlinear Schrödinger (SNLS) equations

$$U_{XX} + g_{11}U^3 + g_{12}UV^2 = 0, \tag{4a}$$
$$V_{XX} + g_{22}V^3 + g_{12}VU^2 = 0, \tag{4b}$$

where g_{11}, g_{12}, and g_{22} are constants, and α_1,α_2,β_1,β_2,X are functions of x and t to be determined. For brevity, we define variables $\sigma_1 = g_{12} - g_{11}$, $\sigma_2 = g_{12} - g_{22}$, and $\sigma_{12} = g_{12}^2 - g_{11}g_{22}$. Substituting Eqs. (3) into Eqs. (2) and asking $U(X)$,$V(X)$ to satisfy Eqs. (4), we have a set of partial differential equations (PDEs). By solving this set of PDEs, we conclude that when

$$b_{11} = g_{11}\theta(t,x), \quad b_{12} = g_{12}\theta(t,x), \quad b_{22} = g_{22}\theta(t,x), \tag{5}$$

with $\theta(t,x) = -\lambda^2 e^{-3\lambda^2x^2-6\lambda\delta x-2\delta^2}/[2\zeta_3^2(t)]$, one has

$$\alpha_1 = \zeta_1(t) - \frac{\lambda_t x^2}{2\lambda} - \frac{\delta_t x}{\lambda}, \quad \alpha_2 = \zeta_2(t) - \frac{\lambda_t x^2}{2\lambda} - \frac{\delta_t x}{\lambda},$$
$$\beta_1 = \beta_2 = \zeta_3(t)e^{\frac{\lambda x(\lambda x+2\delta)}{2}}, \quad X = \frac{\sqrt{\pi}}{2}\mathrm{erf}(\lambda x+\delta), \tag{6}$$

where $\mathrm{erf}(s) = \frac{2}{\sqrt{\pi}}\int_0^s e^{-\tau^2}d\tau$ is called an error function, $\zeta_1(t)$,$\zeta_2(t)$, and $\zeta_3(t)$ satisfy

$$\zeta_1(t) = \int(\lambda^4 - {\delta_t}^2 + \lambda^4\delta^2)/(2\lambda^2)dt + C_1,$$
$$\zeta_2(t) = \int(\lambda^4 - {\delta_t}^2 + \lambda^4\delta^2)/(2\lambda^2)dt + C_2, \quad \zeta_3(t) = \sqrt{\lambda}e^{\frac{1}{2}\delta^2},$$

with C_1 and C_2 arbitrary constants, and λ,δ satisfy

$$\lambda^6 - \gamma^2\lambda^2 - 2{\lambda_t}^2 + \lambda_{tt}\lambda = 0, \tag{7a}$$
$$2\delta_{tt}\lambda + 2\lambda^5\delta - 4\delta_t\lambda_t = 0. \tag{7b}$$

When setting $\sigma_1/\sigma_{12} > 0$ and $\sigma_2/\sigma_{12} > 0$, Eqs. (4) have two families of exact solutions as

$$U^{(1)}(X) = \sqrt{\sigma_2/\sigma_{12}}\nu_1\mathrm{cn}(\nu_1X,\sqrt{2}/2), \tag{8a}$$
$$V^{(1)}(X) = \sqrt{\sigma_1/\sigma_{12}}\nu_1\mathrm{cn}(\nu_1X,\sqrt{2}/2), \tag{8b}$$

and

$$U^{(2)}(X) = \sqrt{2}/2\sqrt{\sigma_2/\sigma_{12}}\nu_2\mathrm{sd}(\nu_2X,\sqrt{2}/2), \tag{9a}$$
$$V^{(2)}(X) = \sqrt{2}/2\sqrt{\sigma_1/\sigma_{12}}\nu_2\mathrm{sd}(\nu_2X,\sqrt{2}/2), \tag{9b}$$

where ν_1,ν_2 are arbitrary constants, $\mathrm{sd} = \mathrm{sn}/\mathrm{dn}$ with sn,cn, and dn being Jacobi elliptic functions. When imposing the bounded condition $\lim_{|x|\to\infty}\psi_{1,2}(x,t) = 0$, we have $\nu_1 = 2(2n+1)K(\frac{\sqrt{2}}{2})/\sqrt{\pi}$ for Eqs. (8) and $\nu_2 = 4mK(\frac{\sqrt{2}}{2})/\sqrt{\pi}$ for Eqs. (9), where n and m are integer numbers and $K(\frac{\sqrt{2}}{2}) = \int_0^{\pi/2}[1-(\frac{\sqrt{2}}{2})^2\sin^2\tau]^{-1/2}d\tau$ is an elliptic integral of the first kind.

After some algebra, we find Eq. (7b) has a solution of the following form:

$$\delta(t) = c_1e^{i\int\lambda^2dt} + c_2e^{-i\int\lambda^2dt}, \tag{10}$$

with c_1 and c_2 arbitrary constants.

Next we set $\lambda = 1/\xi$ to rewrite Eq. (7a) in the form of the Ermakov-Pinney equation [16,17] as

$$\xi_{tt} + \gamma^2\xi = 1/\xi^3. \tag{11}$$

According to the result [17], to obtain the explicit solutions of Eq. (11) we choose γ to satisfy

$$\gamma^2 = \gamma_0^2 + \epsilon\cos(\gamma_1t), \tag{12}$$

with $\epsilon \in (-1,1)$ and $\gamma_0,\gamma_1 \in \mathbb{R}$. Therefore, the general solution to Eq. (7a) is

$$\lambda = \left(A\xi_1^2 + B\xi_2^2 + 2C\xi_1\xi_2\right)^{-1/2}, \tag{13}$$

where A,B,C are constants satisfying $AB - C^2 = 1/W^2$, and the Wronskian $W = \xi_1\xi_{2t} - \xi_2\xi_{1t}$ with (ξ_1,ξ_2) being two linearly independent solutions of a homogeneous ordinary differential equation

$$\xi_{tt} + \gamma^2\xi = 0. \tag{14}$$

Combining Eqs. (3) and (6) with (8) and (9), we arrive at two families of explicitly exact solutions for the coupled quasi-1D GP equations (2) as

$$\psi_1^{(j)}(x,t) = \sqrt{\lambda}e^{\frac{1}{2}\delta^2}e^{\frac{\lambda x(\lambda x+2\delta)}{2}}e^{i\alpha_1(x,t)}U^{(j)}(X), \tag{15a}$$

$$\psi_2^{(j)}(x,t) = \sqrt{\lambda}e^{\frac{1}{2}\delta^2}e^{\frac{\lambda x(\lambda x+2\delta)}{2}}e^{i\alpha_2(x,t)}V^{(j)}(X), \tag{15b}$$

where $U^{(j)}(X)$ and $V^{(j)}(X)$ are given by Eqs. (8) and (9), index $j = 1,2$, α_1,α_2 satisfy Eq. (6), and X,δ,λ satisfy Eqs. (6), (10), and (13), respectively. It is easy to check that $\lim_{|x|\to\infty}\psi_{1,2}^{(j)}(x,t) = 0$ for $j = 1,2$, so these two families of exact solutions are localized nonlinear wave solutions.

IV. DYNAMICS OF THE EXACT LOCALIZED NONLINEAR MATTER WAVES

In this section we discuss the dynamics and important physical applications of the exact localized nonlinear wave solutions (15) of the coupled quasi-1D GP equations (2). We also propose how to control dynamics of localized nonlinear waves in the two-component BECs by the harmonic potentials and the spatiotemporal inhomogeneous s-wave scattering lengths in future experiments.

Similar to the single BECs cases [14], considering different choices of the parameters ϵ, γ_0, and γ_1 in Eq. (12), we can also single out several different types of soliton behaviors, such as breathing solitons, resonant solitons, quasiperiodic solitons, and moving solitons. Here we discuss the existence regions of the exact localized nonlinear matter waves by assuming the two constraint conditions $\sigma_1/\sigma_{12} > 0$ and $\sigma_2/\sigma_{12} > 0$ in Eqs. (8) and (9). Without loss of generality, we always assume $g_{11} > g_{22}$. So we have four cases of parameters g_{11}, g_{22}, and g_{12} as given in the following:

Case 1. $g_{11} > g_{22} > 0$ and $g_{12} > g_{11}$.
Case 2. $g_{11} > g_{22} > 0$ and $\sqrt{g_{11}g_{22}} > g_{12} > -\sqrt{g_{11}g_{22}}$.
Case 3. $g_{22} < g_{11} < 0$ and $g_{12} > \sqrt{g_{11}g_{22}} > 0$.
Case 4. $g_{11} > 0, g_{22} < 0$ and $g_{12} > g_{11}$.

These correspond to four cases of the intracomponent interaction parameters b_{11}, b_{22}, and intercomponent interaction parameters b_{12} [see Eq. (5)] as follows:

Case a. $b_{11} < b_{22} < 0$ and $b_{12} < b_{11}$.
Case b. $b_{11} < b_{22} < 0$ and $-\sqrt{b_{11}b_{22}} < b_{12} < \sqrt{b_{11}b_{22}}$.
Case c. $b_{22} > b_{11} > 0$ and $b_{12} < -\sqrt{b_{11}b_{22}}$.
Case d. $b_{11} < 0$, $b_{22} > 0$, and $b_{12} < b_{11}$.

This demonstrates the regions where the exact localized nonlinear matter waves of the two-component BECs can exist when the intracomponent interaction parameters b_{11}, b_{22}, and intercomponent interaction parameters b_{12} are spatiotemporally inhomogeneous. Cases a and b show that the two-component BEC with two self-attractive atom-atom interactions supports the exact localized nonlinear matter waves, which is similar to the single-component one [14]. However, for cases c and d, it is surprising to see that the exact novel localized nonlinear matter waves can be formed in the two-component BECs with self-repulsive atom-atom interactions. This is because in the two-component BECs, the attractive interactions from the intercomponent interaction b_{12} (see case c), the second component (see case d), or both, induce an effective attractive interaction in the self-repulsive one.

Now we only consider case c, which denotes two self-repulsive atom-atom interactions and attractive intercomponent interactions. The other cases can be studied in the same way. Let us first provide the experimental parameters for producing the quasi-1D two-component condensates composed of $N_1 = N_2 = 5 \times 10^4$ ^{87}Rb atoms [6,18], confined in a cigar-shaped trap, with the ratio of the confining frequencies, $\gamma = \omega_x/\omega_\perp$ of order $O(10^{-2})$. Typically, we choose axial frequency $\omega_x = 70\pi$ Hz and radial frequency $\omega_\perp = 800\pi$ Hz [19]. Then when taking the scattering lengths a_{ij} to be of the order of nanometer, it turns out that the normalized trap strength γ is typically of order $O(10^{-2})$. The behavior of the scattering lengths near a Feshbach resonant magnetic field B_0 is typically of the form $a_s(B) = a[1 + \Delta/(B_0 - B)]$, with a being the asymptotic value of the scattering length far from the resonance, B_0 being the resonant value of the magnetic field, and Δ being the width of the resonance. In our case, the scattering lengths are space and time dependent, i.e., $a_{ij} = a_{ij}(x,t)$, so the magnetic field B that we will use should vary following the space and time. In real experiments, such magnetic field may be generated by a microfabricated ferromagnetic structure integrated on an atom chip [20]. In the following, within the safe region we will always take the parameters g_{ij} in Eq. (5) to be $g_{11} = -1$, $g_{22} = -3$, $g_{12} = 2$.

A. Breathing solitons

In order to investigate the dynamics of the explicitly exact solutions (15), we take special parameters γ_0,γ_1, and ϵ in Eq. (12). When the ratio of the confining frequencies γ of the harmonic potential is time independent, that is, parameters $\gamma_1 = \epsilon = 0$, by solving Eq. (14) we have $\lambda = 1/\xi$ with $\xi = [A - (A - B)\cos^2(\gamma_0 t) + \sqrt{AB\gamma_0^2 - 1}\sin(2\gamma_0 t)/\gamma_0]^{1/2}$. Here ξ is the width of the explicitly exact solutions (15) and $\sqrt{\lambda}$ is its amplitude. We further suppose $c_1 = c_2 = 0$, i.e., $\delta = 0$. When the cigar-shaped trap with axial frequency $\omega_x = 70\pi$ Hz and radial frequency $\omega_\perp = 800\pi$ Hz is considered, the ratio of the confining frequencies $\gamma = \omega_x/\omega_\perp = 7/80$. So from Eq. (12) the parameter $\gamma_0 = \gamma = 7/80$. In order to determine parameters A and B in Eq. (13), we further consider the initial condition of Eq. (11) as $\xi(0) = \sqrt{3}$ and $\xi_t(0) = 1/80$.

We now investigate how the time- and space-modulated nonlinearities b_{ij} control the dynamics of the localized nonlinear matter waves. In the case of parameters $\gamma_1 = \epsilon = \delta = 0$, the nonlinearities in Eq. (2) become $b_{11} = g_{11}\theta(t,x)$, $b_{12} = g_{12}\theta(t,x)$, $b_{22} = g_{22}\theta(t,x)$ with $\theta(t,x) = -\frac{\lambda}{2}e^{-3\lambda^2x^2}$, which are space-localized and time-periodic Gaussian nonlinearity, as shown in Fig. 1. In all figures of this paper, the units of space length and time are 5.34 μm and 0.4 ms, respectively. In real BECs experiments, the Gaussian nonlinearity can be

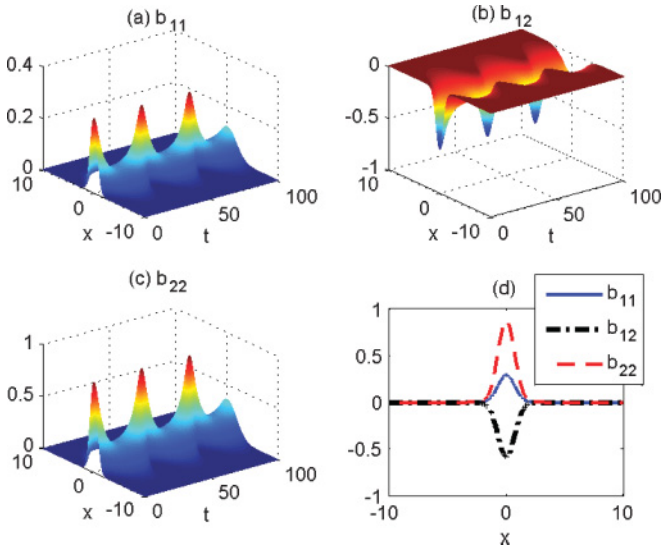

FIG. 1. (Color online) (a)–(c) demonstrate the examples of spatiotemporal-dependent nonlinearities b_{11}, b_{12}, and b_{22} given by Eq. (5) with parameters $g_{11} = -1$, $g_{22} = -3$, $g_{12} = 2$, $\gamma_1 = \epsilon = 0$, and $\gamma_0 = 7/80$. (d) demonstrates the nonlinearities b_{11}, b_{12}, and b_{22} for $t = 0$. Here and after, the units of space length and time are 5.34 μm and 0.4 ms, respectively.

generated by controlling the Feschbach resonances optically or magnetically using a Gaussian beam.

In Fig. 2, we show the evolution of condensate density of the wave functions $\psi_1^{(1)}$ and $\psi_1^{(2)}$ in (15) with the above parameters. The density profiles of the other component $\psi_2^{(1)}$ and $\psi_2^{(2)}$ can also be plotted in the same way, which is similar to that of $\psi_1^{(1)}$ and $\psi_1^{(2)}$ with different amplitudes. Figures 2(a) and 2(b) demonstrate the density profiles of the wave function $\psi_1^{(1)}$ for $n = 0,1$, respectively, and Figs. 2(c) and 2(d) demonstrate the density profiles of the wave function $\psi_1^{(2)}$ for $m = 1,2$, respectively. Figure 2(e) demonstrates the width $\xi = 1/\lambda$ and amplitude $\sqrt{\lambda}$ of the wave functions. It is observed that the localized nonlinear matter waves are space localized and time periodic, which are usually called breathing solitons. Therefore, we have constructed some exact multisoliton breathing solutions of the quasi-1D two-component BECs. Here n and m are the order of the breathing solitons. It is also observed that the amplitude and width of the localized nonlinear matter waves vary periodically with respect to time.

B. Quasibreathing solitons

When the ratio of the confining frequencies γ of the harmonic potential is time dependent, we can select proper parameters γ_0, γ_1, and ϵ in Eq. (12) to formulate a type of quasibreathing solitons in the two-component BECs. We especially choose parameters $\gamma_0 = 7/80$, $\gamma_1 = \sqrt{2}$, and $\epsilon = 1/2$. In this case, the two solutions of Eq. (14) are Mathieu functions $\xi_1 = C_M(49/3200, -1/2, \sqrt{2}t/2)$, $\xi_2 = S_M(49/3200, -1/2, \sqrt{2}t/2)$, where C_M and S_M refer to the cosine and sine Mathieu functions, respectively, which are in the stability region of Eq. (14). With these in mind, we can construct the function λ from Eq. (13). In this section we still assume parameter $\delta = 0$. To determine the unknown

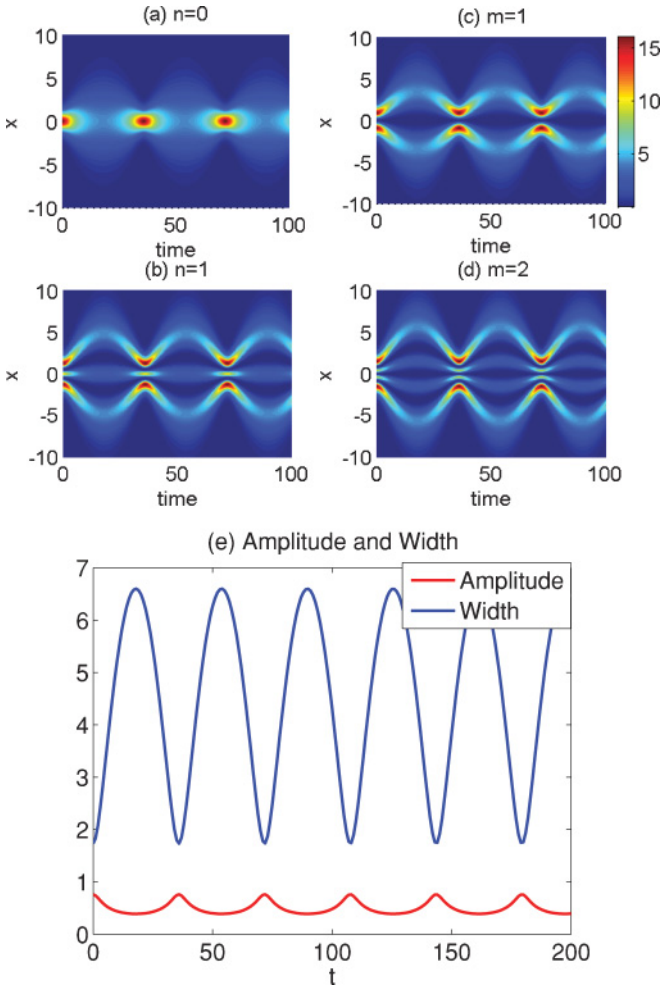

FIG. 2. (Color online) Dynamics of breathing solitons in two-component BECs in quadratic potential with spatiotemporal-dependent nonlinearities shown in Fig. 1. (a) and (b) demonstrate the evolution of condensate density $|\psi_1^{(1)}|^2$ for order $n = 0$ and 1, respectively. (c) and (d) demonstrate examples of condensate density $|\psi_1^{(2)}|^2$ for order $m = 1$ and 2, respectively. (e) demonstrates the width $\xi(t) = 1/\lambda(t)$ (upper line) and amplitude $\sqrt{\lambda(t)}$ (lower line) of wave functions. The parameters are $\gamma_1 = \epsilon = c_1 = c_2 = 0$ and $\gamma_0 = 7/80$. The initial data for Eq. (11) are $\xi(0) = \sqrt{3}$ and $\xi_t(0) = 1/80$.

parameters A and B in λ, we consider the initial condition of Eq. (11) to be $\xi(0) = \sqrt{3}$ and $\xi_t(0) = \sqrt{6}/6$.

In this case, the nonlinearities in Eq. (2) are still space and time dependent and the external potential is time dependent. Next we study how these nonlinearities control the dynamics of the the localized nonlinear matter waves. In Fig. 3 we show the development of density profiles for the wave functions $\psi_1^{(1)}$ and $\psi_2^{(2)}$ in (15). The density profiles of the wave functions $\psi_1^{(2)}$ and $\psi_2^{(1)}$ can also be plotted in the same way, which is very similar to that of $\psi_1^{(1)}$ and $\psi_2^{(2)}$ except the amplitudes. Figures 3(a) and 3(b) demonstrate the density profiles of the wave functions $\psi_1^{(1)}$ for order $n = 0$, and Figs. 3(c) and 3(d) demonstrate the density profiles of the wave functions $\psi_2^{(2)}$ for order $m = 1$. It is observed that the localized nonlinear matter waves are space localized and time quasiperiodic, which are quasibreathing solitons with orders n or m. We

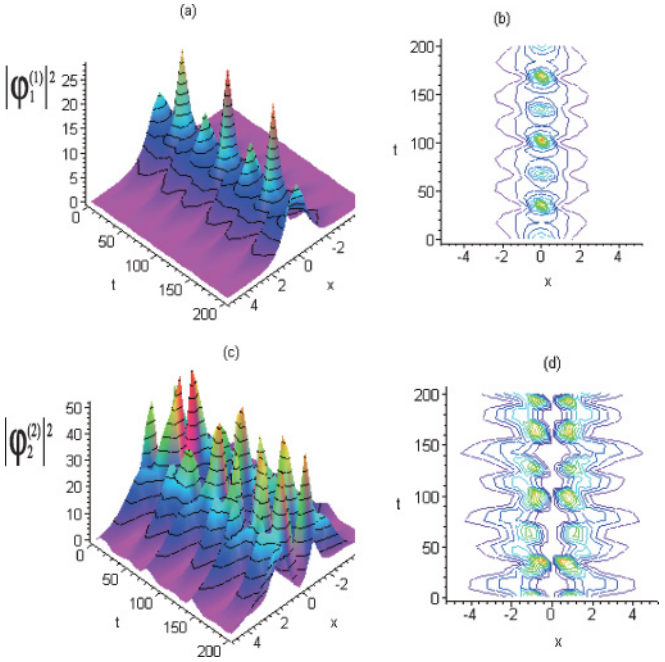

FIG. 3. (Color online) Examples of quasibreathing solitons in two-component BECs in quadratic potential with spatiotemporal-dependent nonlinearities in Eq. (5). (a) and (b) demonstrate the evolution of condensate density $|\psi_1^{(1)}|^2$ for order $n = 0$. (c) and (d) demonstrate the evolution of condensate density $|\psi_2^{(2)}|^2$ for order $m = 1$. The parameters are $c_1 = c_2 = 0$, $\gamma_0 = 7/80$, $\gamma_1 = \sqrt{2}$, and $\epsilon = 1/2$. The initial data for Eq. (11) are $\xi(0) = \sqrt{3}$ and $\xi_t(0) = \sqrt{6}/6$.

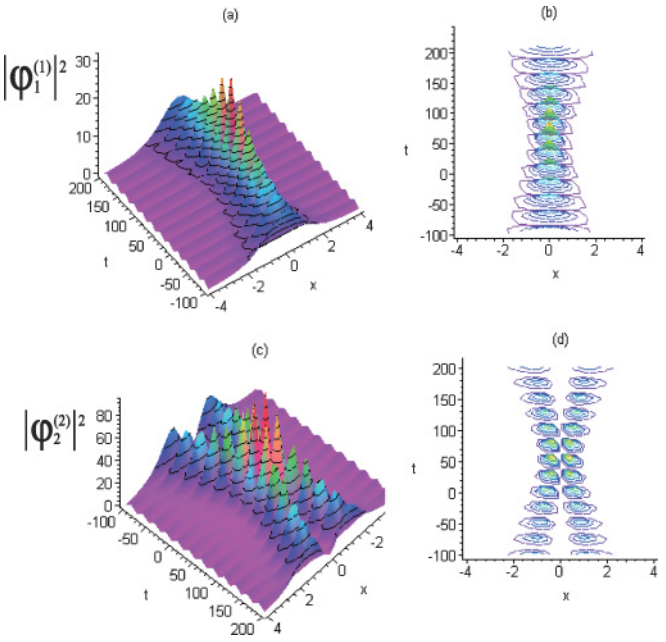

FIG. 4. (Color online) Examples of resonant solitons in two-component BEC in quadratic potential with spatiotemporal-dependent nonlinearities in Eq. (5). (a) and (b) describe the evolution of condensate density $|\psi_1^{(1)}|^2$ for order $n = 0$. (c) and (d) describe the evolution of condensate density $|\psi_2^{(2)}|^2$ for order $m = 1$. The parameters here are $c_1 = c_2 = 0$, $\gamma_0 = 7/80$, $\gamma_1 = 4$, and $\epsilon = 1/2$. The initial data for Eq. (11) are $\xi(0) = 1$ and $\xi_t(0) = 1$.

have constructed some exact quasibreathing soliton solutions of the quasi-1D two-component BECs. It is also observed that the amplitude and width of the quasibreathing solitons vary quasiperiodically with respect to time.

C. Resonant solitons

If we let the parameters $\delta = 0$, $\gamma_0 = 7/80$, $\gamma_1 = 4$, and $\epsilon = 1/2$, we are in the instability region of Eq. (11). However, the solutions of Eq. (14) are also Mathieu functions $\xi_1 = C_M(49/25600, -1/16, 2t), \xi_2 = S_M(49/25600, -1/16, 2t)$. After some algebra, we can also get the analytical expression of function λ. In order to determine the unknown parameters A and B in λ, we consider the initial condition of Eq. (11) as $\xi(0) = 1$ and $\xi_t(0) = 1$.

Figures 4(a) and 4(b) and 4(c) and 4(d) describe the evolution of the condensate density profiles for the wave functions $\psi_1^{(1)}$ with order $n = 0$ and $\psi_2^{(2)}$ with order $m = 1$, respectively. It is shown that the density wave packets are space localized and time resonant, which have the behaviors of resonant solitons. At the beginning, resonant solitons are localized nonlinear matter waves with low amplitude and large width. After some time, their amplitudes become high but widths become small; as time goes on their amplitudes decrease and the widths increase gradually. The nonlinear matter waves demonstrate transitory resonant soliton behaviors. These resonant soliton behaviors come from the coaction of the time-dependent harmonic potential and the spatiotemporal inhomogeneous interactions.

D. Moving solitons

Finally, we consider the case of $\delta \neq 0$, which will produce more nonlinear matter waves. The time-dependent function δ can be determined by Eq. (10) with Eq. (13). In this case, the nonlinearities in Eq. (2) become more complicated, the amplitude of the nonlinear matter wave seems more complex, i.e., $\sqrt{\lambda}e^{\frac{1}{2}\delta^2}$, and the center of the solitons can move following the time because of variable $X = \frac{\sqrt{\pi}}{2}\mathrm{erf}(\lambda x + \delta)$. So for $\delta \neq 0$, our localized nonlinear matter waves are localized moving solitons. By choosing different parameters γ_0, γ_1, and ϵ one can again derive moving breathing soliton solutions, moving quasibreathing soliton solutions, and moving resonant soliton solutions of the quasi-1D two-component BECs (2).

For brevity, we assume the ratio of the confining frequencies γ of the harmonic potential is time independent to show the dynamics of the moving breathing solitons. To do so, we still choose $\gamma_0 = 7/80$ and $\gamma_1 = \epsilon = 0$.

Figures 5(a) and 5(b) describe the evolution of the density profiles for the wave function $\psi_1^{(1)}$ with orders $n = 0, 1$, respectively, and Figs. 5(c) and 5(d) describe the evolution of the density profiles for the wave function $\psi_1^{(2)}$ with orders $m = 1, 2$, respectively. Figure 5(e) demonstrates the shapes of the function $\sqrt{\lambda}$, the width $\xi = 1/\lambda$, and the amplitude $\sqrt{\lambda}e^{\frac{1}{2}\delta^2}$ of the moving breathing solitons. It is found that the localized nonlinear matter waves are space localized and time periodically moving. The amplitude and width of the localized nonlinear matter waves vary periodically with respect to time. It is also observed that the amplitudes of the moving breathing solitons are higher than the breathing solitons in Fig. 2.

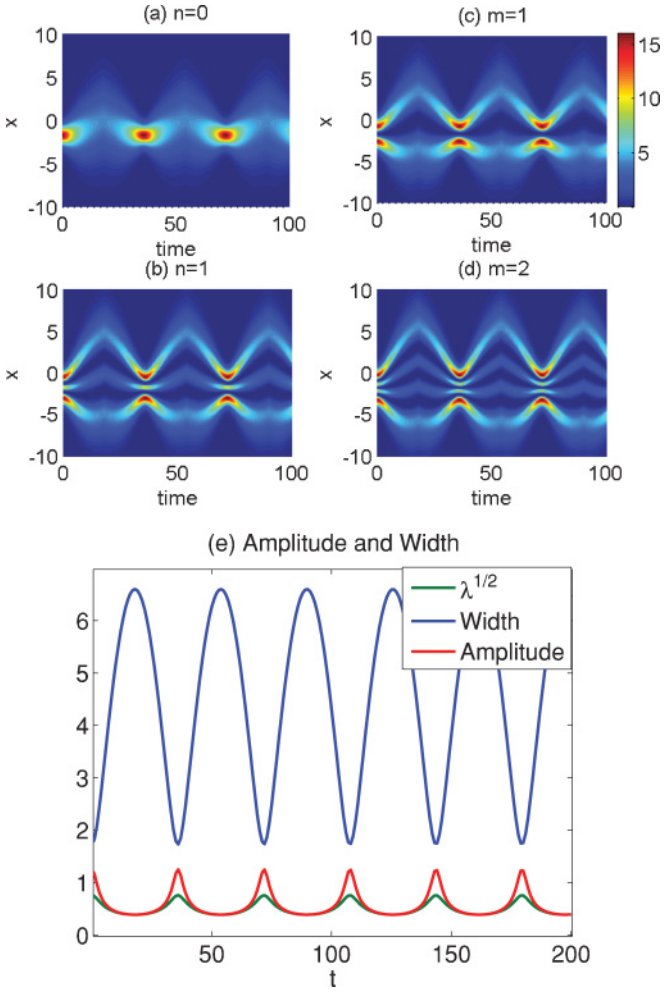

FIG. 5. (Color online) Dynamics of moving breathing solitons in two-component BECs in a quadratic potential with spatiotemporal-dependent nonlinearities in Eq. (5). (a) and (b) describe the evolution of condensate density $|\psi_1^{(1)}|^2$ for order $n = 0$ and 1, respectively. (c) and (d) describe the examples of condensate density $|\psi_1^{(2)}|^2$ for order $m = 1$ and 2, respectively. (e) describes the width $\xi(t) = 1/\lambda(t)$ (upper line), amplitude $\sqrt{\lambda(t)}e^{\frac{\delta^2}{2}}$ (middle line), and function $\sqrt{\lambda(t)}$ (lower line). The parameters are the same as those in Fig. 2 except for $c_1 = c_2 = 1/2$.

V. RESULTS OF NUMERICAL SIMULATIONS

In this section we study the coupled GP equations (2) numerically. First, the dynamical stability of the exact localized nonlinear wave solutions (15) in response to perturbation by initial stochastic noise is done by direct numerical simulations.

Figures 6(a) and 6(b) show the numerical results for the evolution of a breathing soliton solution (15) for $j = 1$ and $n = 0$ with initial Gaussian noise. The other parameters are $g_{11} = 1, g_{22} = -3, g_{12} = 5, \gamma_0 = 7/80, \gamma_1 = \epsilon = 0$, and $c_1 = c_2 = 0$, i.e., $\delta = 0$. Figures 7(a) and 7(b) show the numerical results for the evolution of a moving breathing soliton solution (15) for $j = 1$ and $n = 0$ also with initial Gaussian noise. The other parameters are the same as Fig. 6 but $c_1 = c_2 = 1/2$, i.e., $\delta \neq 0$. Here the Gaussian noise is included by adding to the first component a Gaussian-distributed random number with mean $1/2$ and unit variance, and the second component with

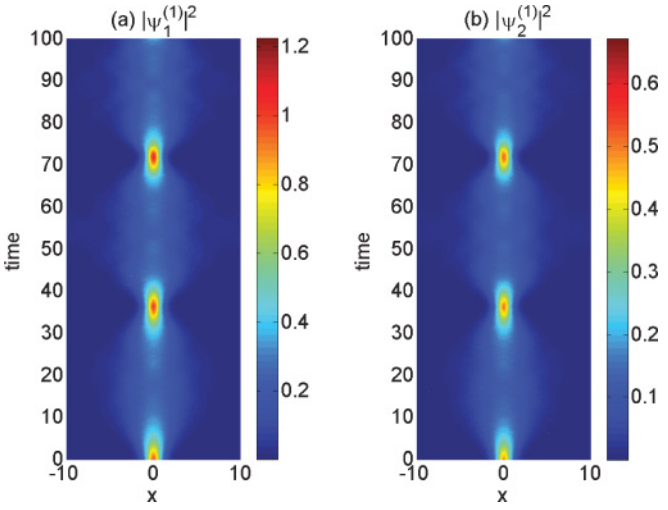

FIG. 6. (Color online) The evolution of a breathing soliton solution (15) for $j = 1$ and $n = 0$ with an initial Gaussian noise of level 5%. The other parameters are $g_{11} = 1, g_{22} = -3, g_{12} = 5, \gamma_0 = 7/80, \gamma_1 = \epsilon = 0$, and $c_1 = c_2 = 0$, i.e., $\delta = 0$.

mean $2/3$ and unit variance multiplied level 5%. It is observed that the exact solution (15) for $j = 1$ and $n = 0$ is dynamically stable for $\delta = 0$, i.e., one order breathing soliton is stable, and the exact solution (15) for $j = 1$ and $n = 0$ is dynamically unstable for $\delta \neq 0$, i.e., one order moving breathing soliton is unstable.

We have tested the dynamical stability of the exact localized nonlinear wave solutions (15) for other parameters by adding certain initial stochastic noises with various intensities, such as Gaussian distributed noise and uniform distribution noise. Our numerical calculations show that only for order $n = 0$ (ground state) is the breathing soliton solution (15) with $\delta = 0$ dynamically stable, while the moving soliton solution (15) with $\delta \neq 0$ is dynamically unstable for all n.

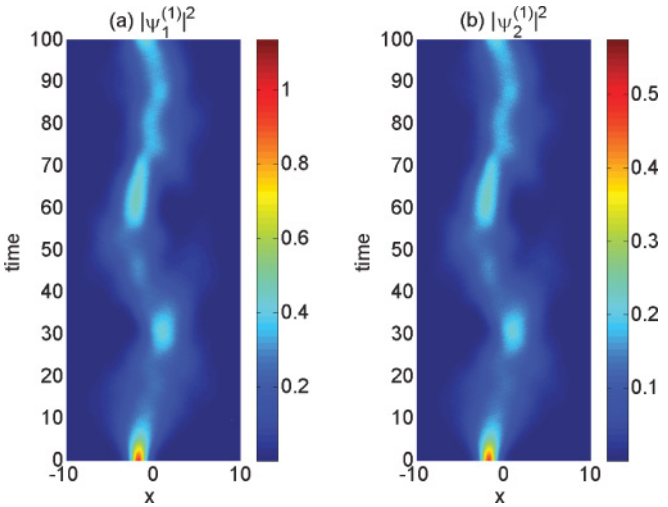

FIG. 7. (Color online) The evolution of a moving breathing soliton solution (15) for $j = 1$ and $n = 0$ with an initial Gaussian noise of level 5%. The other parameters are $g_{11} = 1, g_{22} = -3, g_{12} = 5, \gamma_0 = 7/80, \gamma_1 = \epsilon = 0$, and $c_1 = c_2 = 1/2$, i.e., $\delta = 0$. It is shown that the moving breathing solitons are unstable.

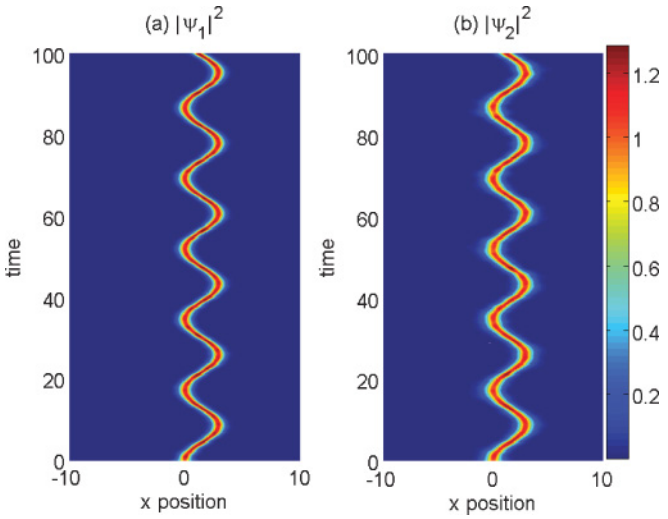

FIG. 8. (Color online) Evolutions of stable vector bright solitons in two-component BECs in quadratic potential with space-periodic nonlinearities $b_{11} = -5\rho, b_{12} = -2\rho, b_{22} = -4.5\rho$, with $\rho = 0.1 + 0.01\sin(x)$.

Second, we illustrate the effect of the general time- and space-modulated nonlinearities on the nonlinear evolution of the condensates. In Sec. III we have shown that the exact localized nonlinear wave solutions (15) exists only for special interaction parameters in Eq. (5). But for other cases of interaction parameters b_{ij}, the coupled GP equations (2) are nonintegrable. Thus we have to appeal to the numerical simulation. Here, we still consider the quasi-one-dimensional geometry characterized by the aspect ratio of the confining frequencies $\gamma = \omega_x/\omega_\perp = 7/80$.

In what follows, we investigate the effect of the interaction parameters $b_{11} = -5\rho$, $b_{12} = -2\rho$, $b_{22} = -4.5\rho$ with three cases of special functions ρ. In the first case, we study the situation in which the scattering lengths are space periodically modulated nonlinearities with $\rho = 0.1 + 0.01\sin(x)$. As shown in Figs. 8, we have performed numerical simulations in the case of the so-called vector bright soliton solutions with initial soliton amplitude $A = 3$ for the first component and $A = 1$ for the second component. It is observed that the space-periodic nonlinearities can support stable snake-shaped vector bright solitons. In the second case, we demonstrate the effect of time-periodic and space-Gaussian nonlinearities with $\rho = 0.1 + 0.01\sin(t)\exp(-x^2)$. It is shown that these nonlinearities can support stable breathing states of the two-component BECs, see Figs. 9. The third case demonstrates the effect of space weakly linear-modulated nonlinearities with $\rho = 0.1 + 0.001x$. As shown in Fig. 10, it is seen that these nonlinearities can also support stable snake-shaped vector bright solitons of the two-component BECs.

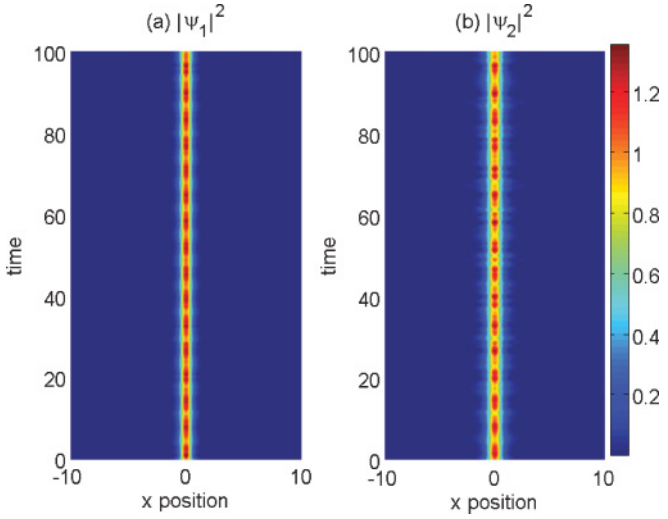

FIG. 9. (Color online) Evolutions of stable breathing states in two-component BECs in quadratic potential with time-periodic and space-Gaussian nonlinearities $b_{11} = -5\rho, b_{12} = -2\rho, b_{22} = -4.5\rho$, with $\rho = 0.1 + 0.01\sin(t)\exp(-x^2)$.

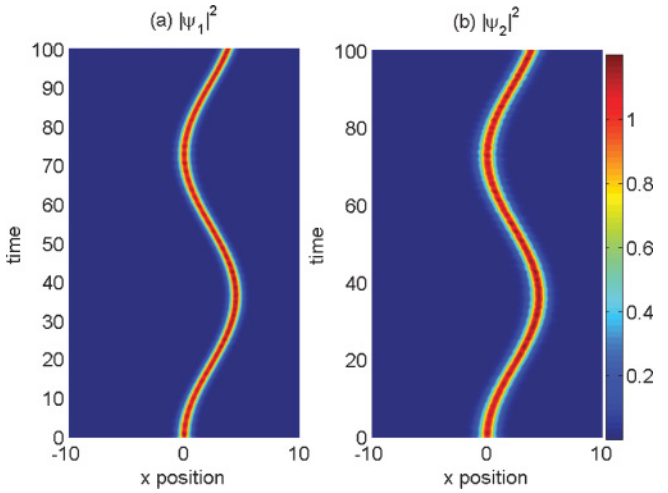

FIG. 10. (Color online) Evolutions of stable vector bright solitons in two-component BECs in quadratic potential with space weakly linear nonlinearities $b_{11} = -5\rho, b_{12} = -2\rho, b_{22} = -4.5\rho$, with $\rho = 0.1 + 0.001x$.

VI. CONCLUSIONS

In conclusion, we have constructed two families of exact solutions of the two-component BECs with spatiotemporal inhomogeneous nonlinearities in a harmonic potential. We show that not only the attractive spatiotemporal inhomogeneous interactions but the repulsive ones support novel localized nonlinear matter waves in two-component BECs. Numerical simulations are used to show the stability of our exact solutions and dynamics of the two-component BECs with general time- and space-modulated nonlinearities. We hope that this research will stimulate further research on those topics and help us to understand the behavior of nonlinear waves in systems with spatially inhomogeneous nonlinearities.

ACKNOWLEDGMENTS

This work was supported by NSFC under Grants No. 10874235, No. 10934010, and No. 60978019, and by NKBRSFC under Grants No. 2006CB921400, No. 2009CB930704, No. 2010CB922904 and No. 2011CB921500. This work was also supported by the China Postdoctoral Science Foundation.

[1] M. H. Anderson *et al.*, Science **269**, 198 (1995); K. B. Davis, M. O. Mewes, M. R. Andrews, N. J. van Druten, D. S. Durfee, D. M. Kurn, and W. Ketterle, Phys. Rev. Lett. **75**, 3969 (1995); C. C. Bradley, C. A. Sackett, and R. G. Hulet, *ibid.* **78**, 985 (1997).

[2] M. R. Matthews, B. P. Anderson, P. C. Haljan, D. S. Hall, C. E. Wieman, and E. A. Cornell, Phys. Rev. Lett. **83**, 2498 (1999); L. Deng *et al.*, Nature (London) **398**, 218 (1999); K. W. Madison, F. Chevy, W. Wohlleben, and J. Dalibard, Phys. Rev. Lett. **84**, 806 (2000); C. Becker *et al.*, Nat. Phys. **4**, 496 (2008).

[3] G. Thalhammer, G. Barontini, L. De Sarlo, J. Catani, F. Minardi, and M. Inguscio, Phys. Rev. Lett. **100**, 210402 (2008).

[4] X. Liu, H. Pu, B. Xiong, W. M. Liu, and J. Gong, Phys. Rev. A **79**, 013423 (2009); X. F. Zhang, X. H. Hu, X. X. Liu, and W. M. Liu, *ibid.* **79**, 033630 (2009); Q. Y. Li, Z. D. Li, L. Li, and G. S. Fu, Opt. Commun. **283**, 3361 (2010); Z.-D. Li and Q.-Y. Li, Ann. Phys. (NY) **322**, 1961 (2007).

[5] K. Kasamatsu and M. Tsubota, Phys. Rev. A **74**, 013617 (2006).

[6] C. J. Myatt, E. A. Burt, R. W. Ghrist, E. A. Cornell, and C. E. Wieman, Phys. Rev. Lett. **78**, 586 (1997).

[7] J. Stenger *et al.*, Nature (London) **396**, 345 (1998).

[8] B. D. Esry, C. H. Greene, J. P. Burke, and J. L. Bohn, Phys. Rev. Lett. **78**, 3594 (1997); T. L. Ho, *ibid.* **81**, 742 (1998).

[9] B. D. Esry and Chris H. Greene, Phys. Rev. A **57**, 1265 (1998); T. Busch, J. I. Cirac, V. M. Perez-Garcia, and P. Zoller, *ibid.* **56**, 2978 (1997); P. Ohberg and S. Stenholm, J. Phys. B **32**, 1959 (1999).

[10] S. Inouye *et al.*, Nature (London) **392**, 151 (1998); J. L. Roberts, N. R. Claussen, J. P. Burke, C. H. Greene, E. A. Cornell, and C. E. Wieman, Phys. Rev. Lett. **81**, 5109 (1998).

[11] F. K. Abdullaev, A. M. Kamchatnov, V. V. Konotop, and V. A. Brazhnyi, Phys. Rev. Lett. **90**, 230402 (2003); X. H. Hu, X. F. Zhang, D. Zhao, H. G. Luo, and W. M. Liu, Phys. Rev. A **79**, 023619 (2009).

[12] J. Belmonte-Beitia, V. M. Perez-Garcia, V. Vekslerchik, and P. J. Torres, Phys. Rev. Lett. **98**, 064102 (2007); H. Sakaguchi and B. A. Malomed, Phys. Rev. E **72**, 046610 (2005).

[13] G. Theocharis, P. Schmelcher, P. G. Kevrekidis, and D. J. Frantzeskakis, Phys. Rev. A **72**, 033614 (2005); M. A. Porter *et al.*, Physica D **229**, 104 (2007); D. A. Zezyulin, G. L. Alfimov, V. V. Konotop, and V. M. Perez-Garcia, Phys. Rev. A **76**, 013621 (2007).

[14] J. Belmonte-Beitia, V. M. Perez-Garcia, V. Vekslerchik, and V. V. Konotop, Phys. Rev. Lett. **100**, 164102 (2008); A. T. Avelar, D. Bazeia, and W. B. Cardoso, Phys. Rev. E **79**, 025602(R) (2009).

[15] D. S. Wang, X. H. Hu, J. Hu, and W. M. Liu, Phys. Rev. A **81**, 025604 (2010).

[16] V. P. Ermakov, Univ. Izv. Kiev **20**, 1 (1880); E. Pinney, Proc. Amer. Math. Soc. **1**, 681 (1950).

[17] R. M. Hawkins and J. E. Lidsey, Phys. Rev. D **66**, 023523 (2002).

[18] K. M. Mertes *et al.*, Phys. Rev. Lett. **99**, 190402 (2007).

[19] K. E. Strecker, J. W. Merrill, R. Carretero-Gonzalez, D. J. Frantzeskakis, P. G. Kevrekidis, and D. S. Hall, Nature (London) **417**, 150 (2002).

[20] M. Vengalattore *et al.*, J. Appl. Phys. **95**, 4404 (2004); Eur. Phys. J. D **35**, 69 (2005).